*International Journal of Research in Engineering and Science (IJRES)*
*ISSN (Online): 2320-9364, ISSN (Print): 2320-9356*
*www.ijres.org Volume 13 Issue 6 ǁ June 2025 ǁ PP. 184-197*

# Numerical Simulation of Multi-Channel Bifurcated Piping System in Underground Wind Turbine Space and Optimization of Construction Technology and Construction Optimization

NIU Rui[1], LI Gang[3], WANG An-yuan[2], LI Nai-yi[3]
[1]*China Railway Tunnel Bureau Group Co., Ltd., Guangzhou 511458*
[2]*China Railway Tunnel Group Second Branch Co., Ltd., Langfang 065000*
[3] *School of Environment and Architecture, University of Shanghai for Science and Technology, Shanghai 200093*

***Abstract***
*This paper examines the safety, stability, and efficiency challenges associated with the construction of complex intersections in the context of the multi-channel bifurcated pipeline system of the underground wind turbine room in the Phase II project of the Suzhou International Rapid Logistics Corrido. Three-dimensional finite element simulation is employed to examine the impact of disparate excavation sequences, lining timings, and pipe interactions on tunnel settlement and structural stability. It was determined that the sequence of expanding the excavation from a large section to a small section can effectively reduce the stress concentration and deformation of the surrounding rock. Furthermore, the lining construction is carried out immediately after the excavation of the wind turbine room, which helps to control the settlement and improve the construction efficiency. Additionally, the up-span ventilation pipeline will have a greater impact on the settlement of the left line of the tunnel on the lower side, which needs to be monitored and supported. Ultimately, an optimized construction plan is proposed, which incorporates the I32 gantry and overrun conduit system to dynamically support a 4-meter-long conduit with a 40-centimeter spacing. This approach aims to ensure the structural stability of the intersection, minimize interference with other passages during construction, and guarantee overall construction safety and long-term stability.*
***Keywords:*** *underground wind turbine room; multi-channel bifurcation; numerical simulation; excavation sequence; perimeter rock deformation; construction optimization*

---

Date of Submission: 12-06-2025 Date of acceptance: 28-06-2025

---

## I. INTRODUCTION

With the rapid development of the national economy and urbanization, the demand for underground infrastructure, such as traffic tunnels and underground wind turbine rooms, has surged. The construction of extra-long and deep tunnels is pushing for larger dimensions and greater depths, imposing higher technical requirements and challenges in design and construction, especially under complex geological conditions where safety, stability, and efficiency are critical concerns [1].

Substantial progress in underground engineering has been made through domestic and international research. Zhang [2] analyzed the mechanics of long highway tunnels with cross-channel intersections, focusing on the impact of intersection angles on rock stress and deformation. Li Chongyang[3] studied rock stability in the underground cavern group of the BTK Hydropower Station, proposing strategies based on ground stress and excavation schemes. Luo Yanbin [4] examined the effects of diagonal cross-passages on deformation and stress concentration in main tunnel linings. Yang Linder [5] investigated rock stability at cavern intersections in the Longtan Hydropower Station. Pan Ting [6] optimized support designs for the Yellow River Tsiha Gorge Hydropower Station's underground cavern group. These studies provide valuable theoretical insights for underground engineering.

However, as extra-long tunnel projects expand, particularly in complex geological conditions, new challenges emerge. Auxiliary structures like inclined shafts, wind turbine rooms, and connection ducts intersect with main caverns, forming complex underground systems such as shaft-cavern transitions, fan room-passage intersections, and substation-main cavern connections [7]. These configurations complicate mechanics, increase excavation difficulties, and heighten spatial effects, revealing gaps in understanding spatial mechanics and dynamic rock behavior.

Numerical simulations play a key role in evaluating mechanical behavior and optimizing excavation and support strategies, especially in large-span, complex layouts under poor geological conditions. This study uses three-dimensional finite element simulations to address the technical challenges in the Suzhou Logistics

Corridor Phase II Project, focusing on optimizing excavation sequences, support systems, and lining construction for enhanced safety and stability [8].

## II. PROJECT OVERVIEW

The Suzhou International Rapid Logistics Corridor Phase II - Yangtze River Road South Extension Project begins north of the Yangtze River Road and Qizi Road intersection and extends south along Yangtze River Road Fig. 1). The route includes a ground-level crossing at Qizi Road and a tunnel passing Baobai West Road, Jinfu Road, and Qizi Mountain, avoiding the Suzhou National Defence Education Centre, Qizi Mountain Landfill, and Cemetery. It connects to Wangshan Road near Huanshan Road and continues as a tunnel under Huanshan Road, Changjiang Road, Wuzhong Avenue, and North Guandu Road, surfacing near South Guandu Road. The total length is 6.428 km, including 6.18 km of tunnel.


**Figure. 1 Project Schematic.**

The duct system of the wind turbine room, as shown in Fig. 2, includes 275 meters of inclined shafts, 75 meters of auxiliary construction passages, 86.15 meters of wind turbine room section, 34 meters of distribution room, 64.95 meters of left-line contact duct, 137.67 meters of right-line contact duct, 40.6 meters of equipment transport passages, 50 meters of maintenance passages in the distribution room, and 52.8 meters of maintenance passages in the wind turbine room.

The underground wind turbine room covers 1481.8 m², comprising a turbine room, power distribution room, contact duct, equipment transport passage, pedestrian maintenance passage, and auxiliary construction passage [9]. It features six passage types, 11 section shapes, and 15 crossing systems, with transitions between small and large sections. These variable-section intersections in narrow spaces pose significant engineering challenges for ensuring multi-chamber construction safety.

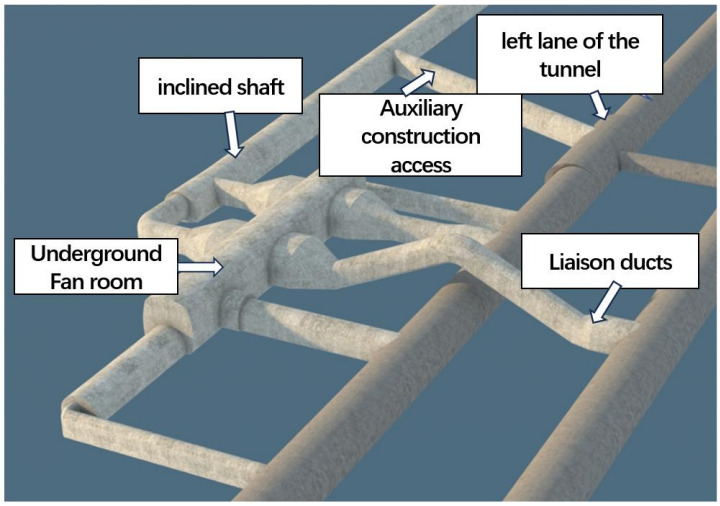


**Figure. 2 Schematic diagram of ductwork in underground fan room.**

A notable difficulty is the contact duct of the right line, which crosses the mainline left tunnel. Its slope reaches 43.6% at the fan room connection and 47.8% at the right line connection, further complicating construction.

## III. FINITE ELEMENT NUMERICAL ANALYSIS OF CONSTRUCTION DIFFICULTIES

Due to the complexity of the tunnelling works, especially the intersection of multiple passages in the underground fan room and the frequent changes in cross sections, the construction faced enormous technical challenges.Therefore, 3D finite element numerical simulation analyses under three major working conditions were carried out to accurately assess the structural forces and deformations at the construction difficulties for this engineering challenge.

### 3.1 underlying assumption

To accurately analyze the impact of the existing tunnel's left line on the excavation of the upper-side contact duct, the effect of different excavation sequences of the fan room flare, and the influence of fan room lining sequences on surrounding tunnels, this study employs large-scale finite element software to simulate the deformation, internal force, and stress characteristics at the intersection of the slanting shaft and main tunnel.

Given the complexity of real-world engineering, the numerical model is based on the following assumptions to improve computational efficiency and minimize the influence of complex factors:

i.The Ducker-Prager yield criterion is used for calculations.

ii.Strata stratification and rock mass joints are neglected, treating the surrounding rock as homogeneous and continuous.

iii.Tectonic stress is excluded; only self-gravity stress is considered in the initial stress field [10].

iv.Groundwater effects are ignored.

v.Excavated materials are modeled as homogeneous elastic-plastic 3D solids Mohr-Coulomb), tunnel support as 2D plates, and anchors as 1D line elements [11].

vi.Boundary constraints include horizontal constraints on the sides, vertical constraints on the base, and free upper boundaries[12].

### 3.2 Model introduction and meshing

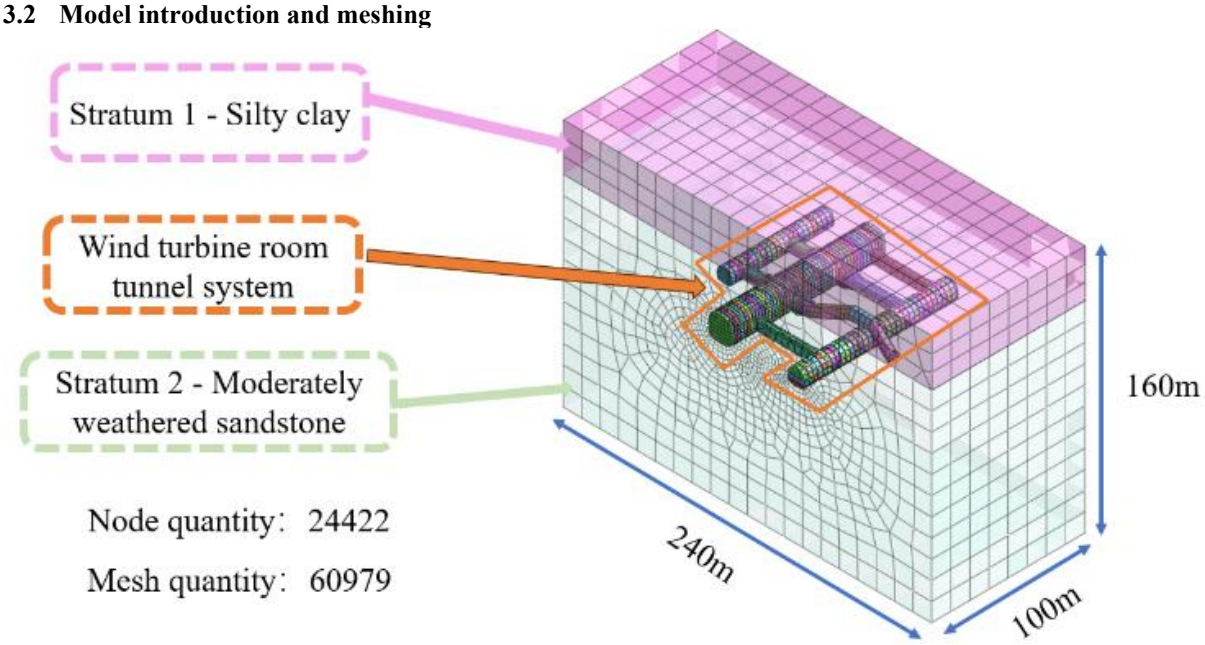


**Figure. 3 Mesh of unexcavated finite element model.**

In this numerical analysis, a stratum structure model was employed, as illustrated in Fig. 3. To minimize boundary effects, the model extends 240 m from the tunnel axis on both sides, 70 m below the tunnel bottom, and to the tunnel's actual burial depth of 47 m above[13]. The excavated soil and surrounding rock were modeled using 3D solid elements.

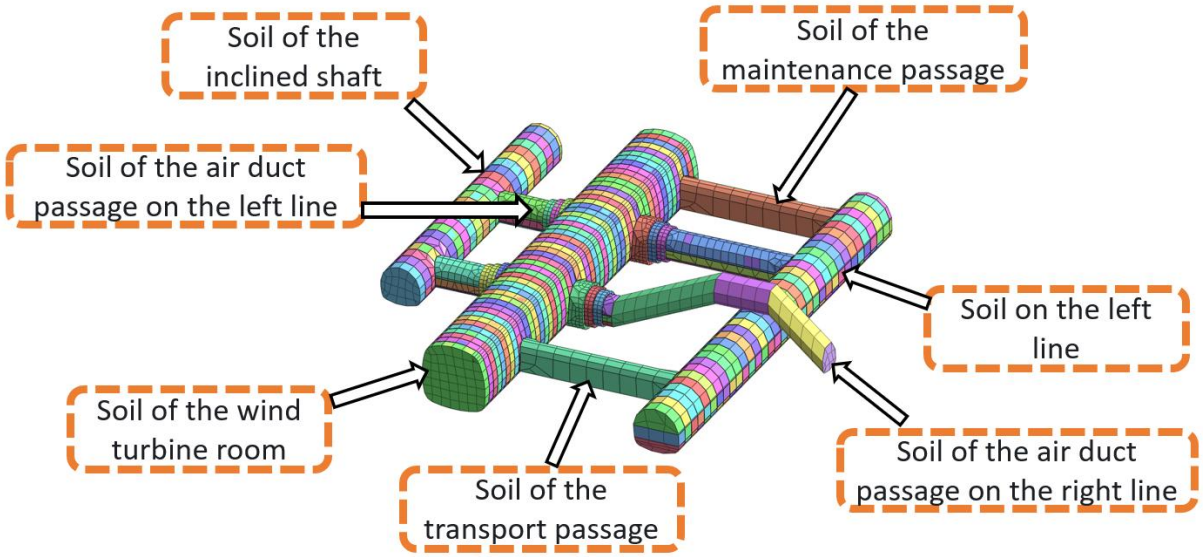


**Figure. 4 Mesh of finite element model for underground wind turbine room and unexcavated tunnel.**

The underground wind turbine room, covering 1,481.8 m², includes caverns such as the turbine room, power distribution room, connecting air duct, equipment transport passage, pedestrian maintenance passage, and auxiliary construction passage. It features six passage types, 11 cross-sectional configurations, and 15 intersection systems [14], located in Grade IV surrounding rock. The spatial layout of the wind turbine room and left and right tunnels is shown in Fig. 4, with the model's physical parameters detailed in Tab. 1.

**Table.1 Physical Parameters of the Model.**

| Earth | Layer thickness m) | Capacity KN/m3) | Modulus of elasticity MPa) | Poisson's ratio | Angle of internal friction °) | Cohesion KPa) |
|---|---|---|---|---|---|---|
| Silty clay | 9.6 | 17.8 | 10.0 | 0.32 | 25 | 50 |
| Moderately weathered sandstone | 10.0 | 20.0 | 18.0 | 0.35 | 31 | 64 |
| Initial support shotcrete | —— | 22.0 | 28000 | 0.20 | —— | —— |
| Pre-stressed anchor bolt | —— | 21.0 | 28000 | 0.20 | —— | —— |

### 3.3 Analysis of Lining Effect in the Wind Turbine Room

As shown in Fig. 5, the maximum displacement of the excavated soil occurs in the lower surrounding rock of the wind turbine room, reaching 1.20 cm. Displacements in the uppermost soil masses of the left-line tunnel, wind turbine room, and inclined shaft are smaller, ranging from 0.27 to 0.35 cm. Displacement increases with depth, rising from 0.43 cm to a maximum of 1.20 cm, located below the intersection of the wind turbine room and ventilation duct. Surrounding ventilation ducts, maintenance passages, and equipment transport passages exhibit relatively uniform displacements, ranging from 0.50 to 0.66 cm.

Fig. 6 reveals that the maximum soil displacement occurs in the lower perimeter rock of the wind turbine room, reaching 0.99 cm, while displacements in the upper soil of the left tunnel, wind turbine room, and inclined shaft remain smaller, between 0.30 and 0.36 cm. As depth increases, soil displacement rises from 0.47 cm to 1.20 cm, peaking beneath the intersection of the fan room and ventilation channel. Displacements in the ventilation ducts, maintenance passages, and equipment transport channels are uniform, ranging from 0.47 to 0.70 cm.

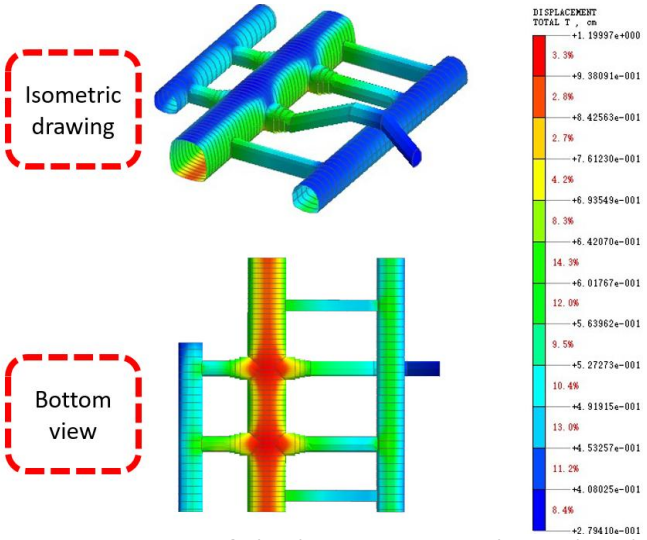


**Figure. 5 Total displacement contour map of pipeline system under immediate lining after wind turbine room excavation.**

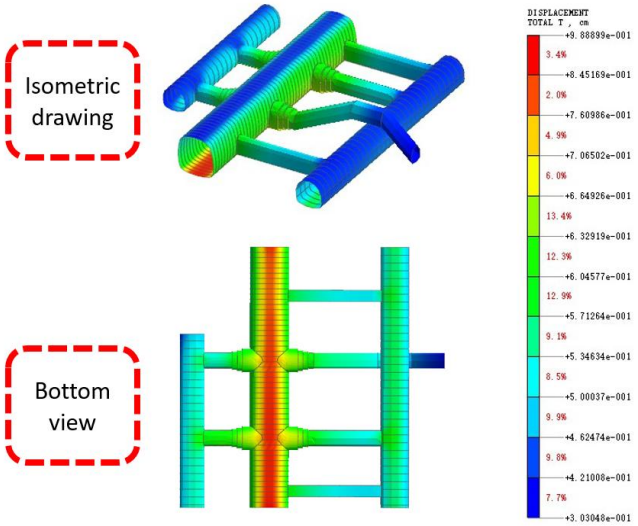


**Figure. 6 Total displacement contour map of pipeline system under lining after construction.**

Comparison with Fig. 5 highlights significant differences under varying construction conditions. Completing the lining after pipeline construction reduces maximum settlement but induces larger displacements in the lower soil of the wind turbine room. Conversely, lining after excavation shifts larger displacements to the fan room-ventilation duct intersection while limiting pipeline system soil displacement.

The layout of measurement line 1, with 15 evenly spaced points along the upper side of the fan room, is shown below（Fig 7）.

Fig.7 and 8 illustrate the variability in settlement displacements at measurement points along measurement line 1. Taking point G5 as an example, the settlement displacement is 0.39 cm when lining is performed after completing the pipeline system construction. In contrast, it decreases to 0.31 cm when lining is conducted immediately after the wind turbine room excavation. A similar trend is observed at point G8, where the settlement displacement is 0.38 cm in the former scenario and 0.31 cm in the latter, highlighting the influence of different construction sequences.

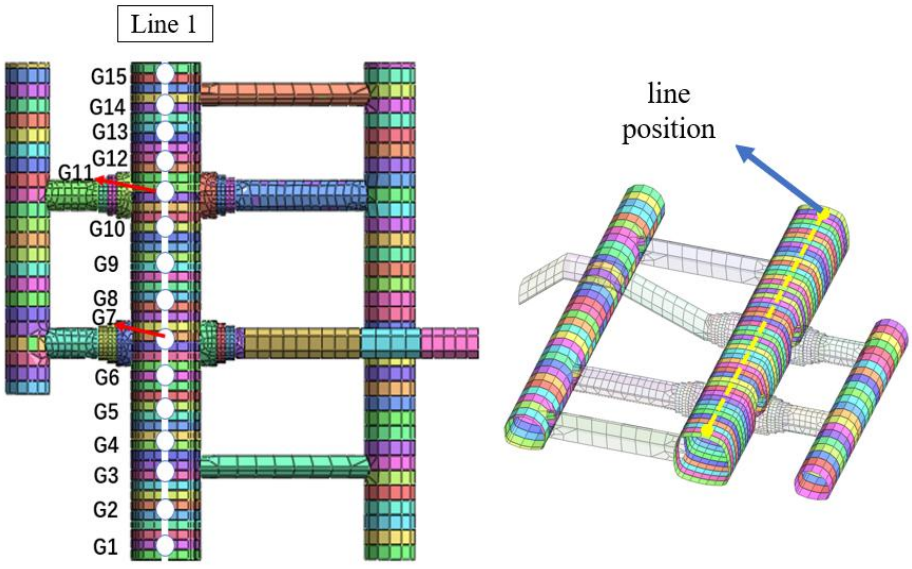


**Figure. 7 Schematic of Line 1 measurement point.**

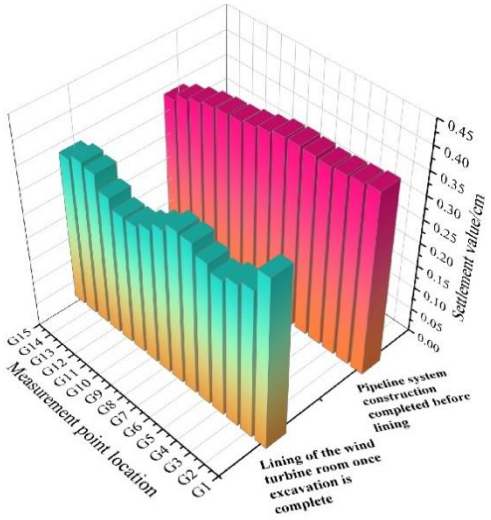


**Figure. 8 Schematic diagram of displacement of survey line 1.**

Further calculations show that the average settlement displacement along measurement line 1 is approximately 0.36 cm when lining is performed after pipeline construction, compared to 0.32 cm when lining follows immediately after wind turbine room excavation. This reduction indicates improved deformation control with the latter approach.

In summary, lining immediately after excavation minimizes displacement and settlement, offering better deformation control and structural stability. Given the wind turbine room's complexity, with its multiple passages and large cavern space, the timing of lining operations is crucial for maintaining stability.

Simulation results confirm that immediate post-excavation lining significantly reduces soil displacement, particularly beneath the wind turbine room. In contrast, lining after pipeline construction, while reducing settlement in specific areas, increases displacement in surrounding soil. Thus, immediate lining post-excavation is the preferred strategy for effective settlement control and overall structural stability.

### 3.4 Right line ventilation duct impact

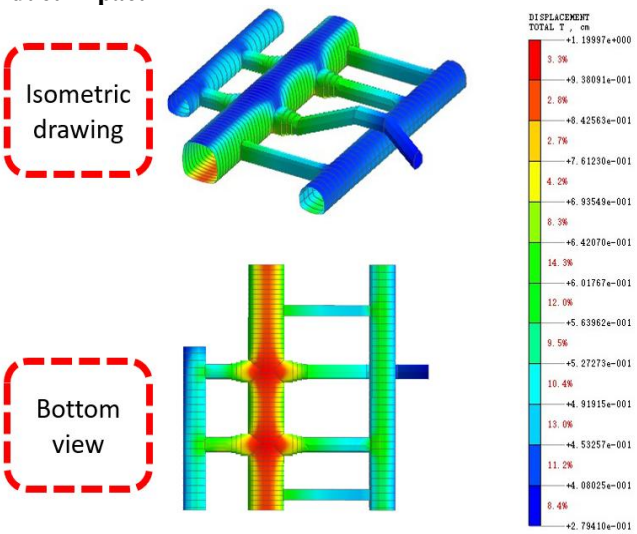


**Figure. 9 Total displacement of piping system considering the case of right-hand line ventilation ducts.**

From Fig. 9, the maximum displacement of the excavated soil occurs in the lower surrounding rock of the wind turbine room, reaching 1.20 cm. In contrast, displacements in the left tunnel, the uppermost soil of the wind turbine room, and the inclined shaft are smaller, ranging from 0.28 to 0.36 cm. Displacement increases with depth, from 0.51 cm to a maximum of 1.18 cm, located beneath the intersection of the fan room and ventilation channel. Displacements in the ventilation ducts, maintenance passages, and equipment transport channels are relatively uniform, between 0.43 and 0.51 cm.

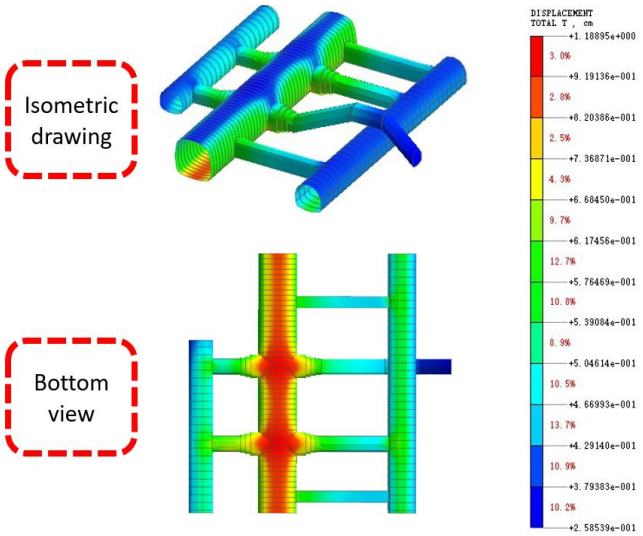


**Figure. 10 Total displacement cloud of the duct system without considering the right line ventilation duct case.**

Fig. 10 similarly shows the maximum displacement in the lower surrounding rock of the wind turbine room, at 1.09 cm. Smaller displacements, ranging from 0.24 to 0.32 cm, are observed in the left tunnel, wind turbine room, and uppermost soil of the inclined shaft. Displacement increases with depth, from 0.45 cm to a maximum of 1.09 cm, also beneath the fan room-ventilation channel intersection. Uniform displacements of 0.38 to 0.45 cm are observed in the ventilation ducts, maintenance passages, and equipment transport channels.

The layout of measurement points of measurement line 2 is as follows, 15 measurement points are evenly arranged on the left side of the tunnel.

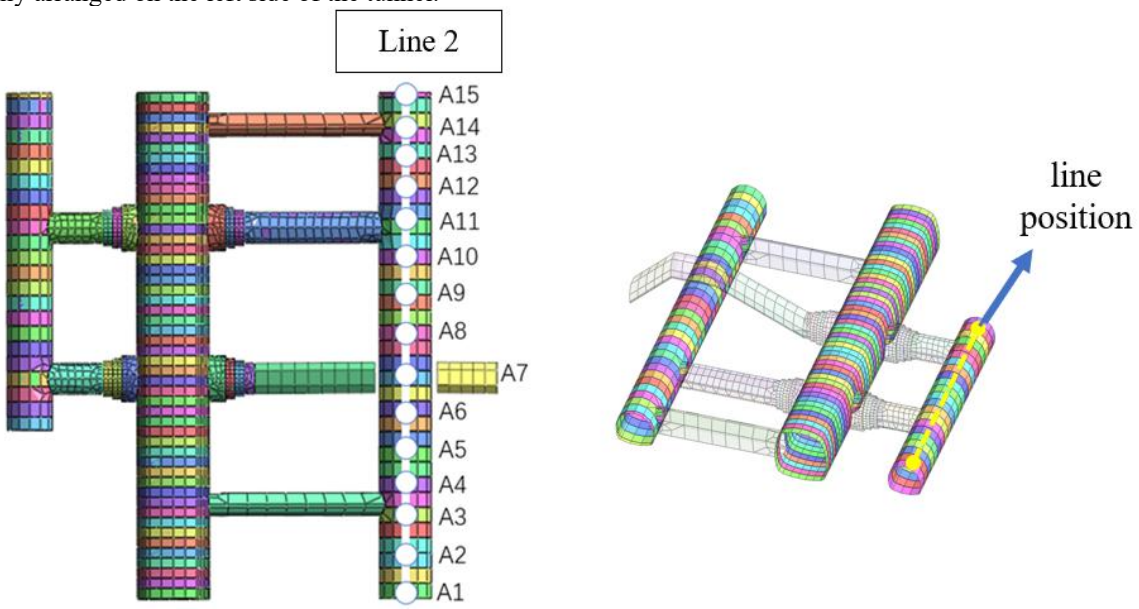


**Figure. 11 Schematic of Line 2 measurement point.**

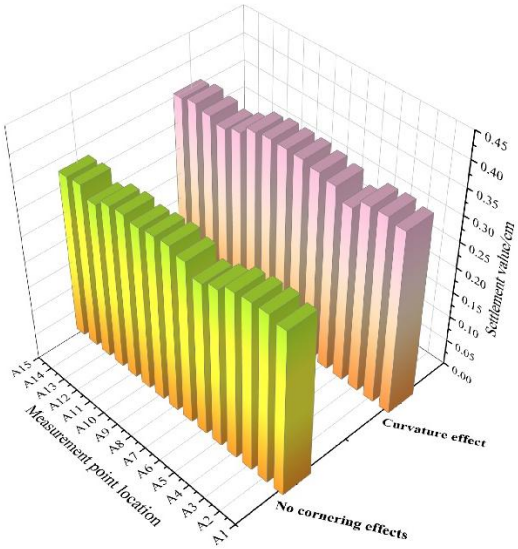


**Figure. 12 Schematic of Line 2 settlement.**

In summary, the settlement impact on the pipeline system is significantly lower when the right-lane ventilation bend is not considered. For Line 2, the average settlement is 0.32 cm without the bends, compared to 0.35 cm with the bends, indicating improved tunnel structure stability in the absence of the bends.

The right ventilation duct notably affects the displacement and settlement of the left tunnel, increasing soil settlement around the left tunnel and surface layers during its construction.

Thus, during the construction of the right-line ventilation duct, it is crucial to enhance support and monitoring around the left tunnel to mitigate its impact on the existing structure.

### 3.5 Analysis of the sequence effect of expanding the excavation

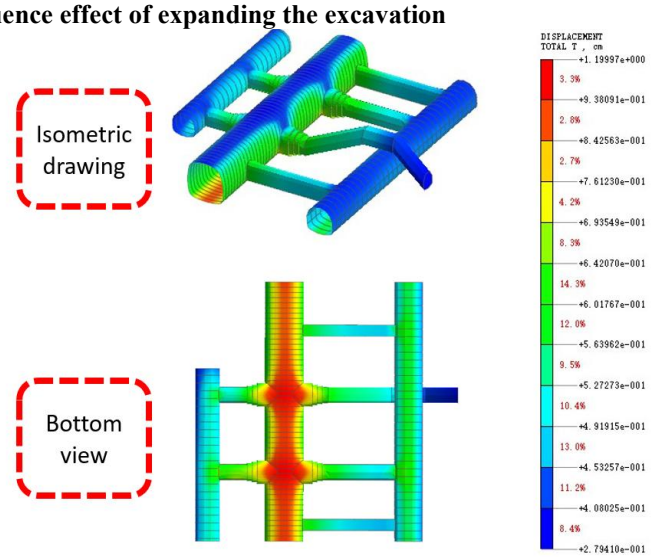


**Figure. 13 Total displacement of piping system under flare condition for small enlarged construction ventilation ducts.**

From Fig. 13, the maximum displacement of the excavated soil occurs in the lower surrounding rock of the wind turbine room, reaching 1.20 cm. In comparison, displacements in the left tunnel, wind turbine room, and uppermost soil of the inclined shaft are smaller, ranging from 0.27 to 0.35 cm. As the excavation depth increases, soil displacement rises from 0.43 cm to a maximum of 1.20 cm, located directly below the intersection of the wind turbine room and the ventilation channel. Displacements in the surrounding ventilation ducts, maintenance passages, and equipment transport channels are more uniform, ranging from 0.50 to 0.66 cm.

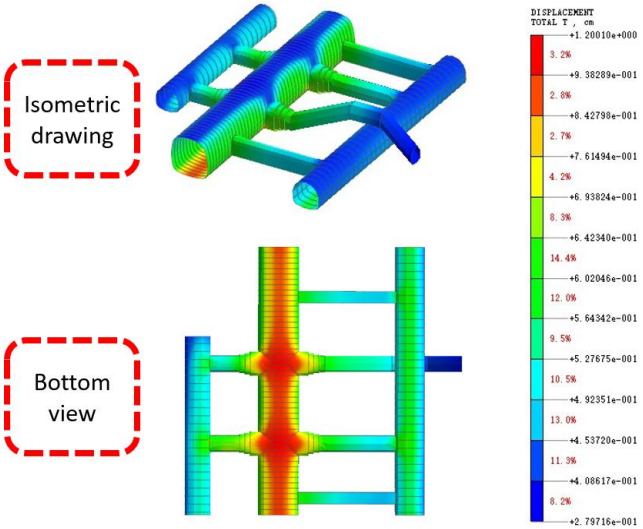


**Figure. 14 Total displacement of piping system under the condition of large and small construction vent flare map.**

From Fig. 14, the maximum displacement of the excavated soil occurs in the lower surrounding rock of the wind turbine room, reaching 1.20 cm. In contrast, the displacement in the left tunnel, wind turbine room, and uppermost soil of the inclined shaft remains relatively small, ranging from 0.27 to 0.35 cm. As depth increases, the displacement of the excavated tunnel soil rises from 0.43 cm to a maximum of 1.20 cm, located directly beneath the intersection of the wind turbine room and the ventilation channel. The displacement in the surrounding ventilation ducts, maintenance passages, and equipment transport channels is uniform, ranging from 0.50 to 0.66 cm.

Measurement points for measurement line 3 are uniformly distributed across 15 points along the upper side of the wind turbine room.

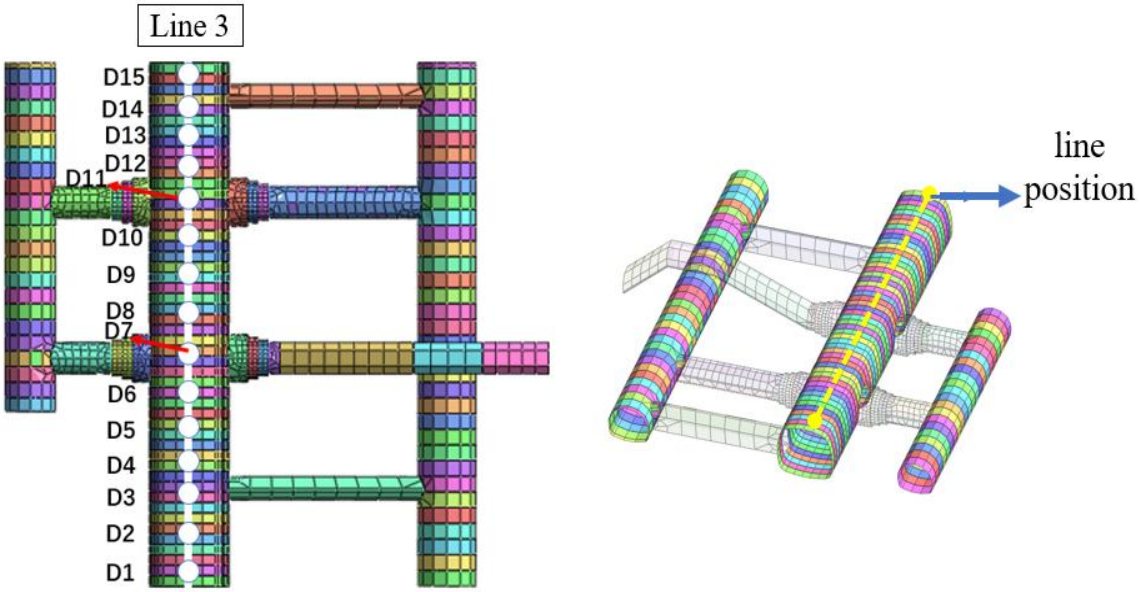


**Figure. 15 Schematic diagram of line 3 measurement points.**

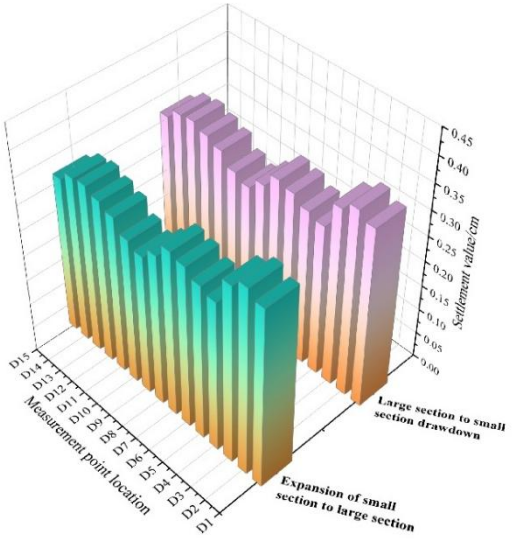


**Figure. 16 Schematic diagram of displacement of survey line 3.**

As shown in Fig. 16, the settlement displacements of measurement line 3 under the two excavation conditions are nearly identical, indicating no significant difference in their impact on the upper side of the ventilator room. However, comparing Fig. 14 and Fig. 15, the large-to-small excavation sequence reduces the displacement of the unexcavated soil around the piping system. Thus, the "big expanding, small construction" method is more effective, as it minimizes displacement, particularly at the intersection of the wind turbine room and the ventilation channel, and enhances surrounding rock stability. Therefore, this excavation method should be prioritized.

## IV. UNDERGROUND WIND TURBINE ROOM MULTI-CHANNEL BIFURCATION INTERSECTION EXCAVATION SUPPORT TECHNOLOGY

The underground ventilator room construction is complex, involving intersecting passages, cross-section transitions, and spatial coordination. At multi-branch intersections, efficient excavation and support are crucial. Based on numerical simulations, this section details excavation steps, support methods, and construction sequences, emphasizing steep gradients and frequent transitions to demonstrate how optimized techniques improve safety, reduce risks, and enhance efficiency.

### 4.1 Wind turbine room excavation construction steps

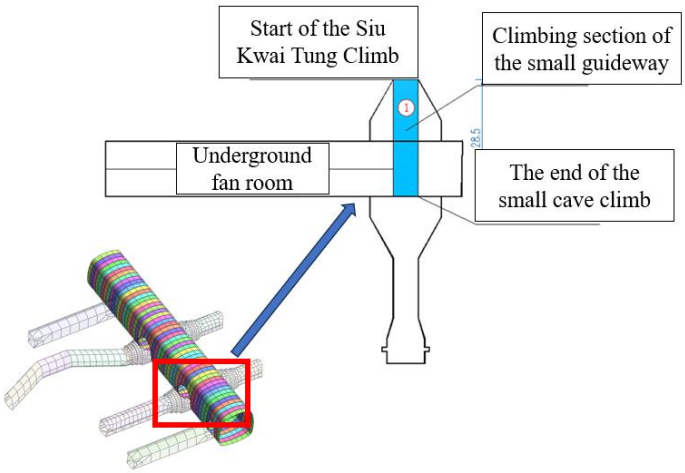


**Figure. 17 Schematic diagram of small guide hole excavation.**

Step 1: After completing the left-line contact duct's normal section, it is used as a small guide tunnel to ascend into the underground wind turbine room Fig. 17). The excavation dimensions are 7.32 m in width, 7.71 m in height, with a climbing slope of 25.8%, and a length of 28.5 m. Support includes Φ6 mm reinforcing steel mesh at 20×20 cm spacing, I14 I-beams at 0.8 m spacing, and Φ42 small conduit pipes L-3.5 m.with locking

anchor tubes on both sides. C22 mm reinforcing steel connecting bars are arranged in a plum-blossom pattern with 1.0 m spacing. The step excavation uses 10 cm thick C25 spray concrete for single sidewall construction[10][11].

Step 2: The small guide tunnel excavation extends into the wind turbine room, completing the excavation and support of the left upper guide tunnel from the climbing point to the end.

Step 3: From the climbing point to the end of the wind turbine room, the upper right guide tunnel, middle left guide tunnel, middle right guide tunnel, lower left guide tunnel, and lower right guide tunnel are expanded and constructed[12].

Step 4: Initial support for the power distribution room is completed using the divided excavation method, followed by second lining construction for unaffected sections of the wind turbine and power distribution rooms.

Step 5: Excavation and support for the left-line main tunnel are completed up to MLK3+158. The equipment transport channel and power distribution room are excavated and supported, with second linings completed. The left-line contact duct is excavated, while the right-side contact duct of the wind turbine room is accessed via the small guide tunnel and excavated by reverse expansion following the design cross-section. Simultaneously, the left contact duct and secondary lining of the equipment transport channel are completed. The left-line tunnel's second lining reaches MLK3+150, while the left-line contact duct's second lining at MLK0+195 to MLK0+205 reaches full strength. Excavation and support for the right-line contact duct proceed to MRK3+160, and when crossing the left-line construction, the superelevation arch bottom is reinforced as per design. The left-line contact tunnel's second lining is completed [14].

Step 6: Excavation and support for the maintenance channels of the power distribution and wind turbine rooms are carried out, followed by second lining construction for the right-line contact duct, power distribution room, and wind turbine room maintenance channels.

### 4.2 Steps for construction of ductwork intersections in a fan room

This paper introduces an optimized construction plan based on numerical analysis, focusing on innovative methods for tunnel intersection construction. The approach emphasizes process coordination and reinforced support systems to ensure structural stability and efficiency.

i.Construction plan for the intersection of the equipment transportation corridor and the underground fan room:

Following the initial support of the left-line main tunnel, construction begins at the equipment transport channel and underground wind turbine room intersection. After completing the underground wind turbine room's initial support and steel arch installation, shotcrete thickness is limited to half the design value 13 cm). During the inverted arch and secondary lining construction, the intersection area is reserved, ensuring the secondary lining of the wind turbine room reaches 100% design strength before formal excavation.

At the intersection, the steel arches and shotcrete along the excavation contour are removed, and I32 gantries are installed. Overrun grouting conduits 42×4 mm, 4.0 m long.are deployed with 40 cm annular spacing. Excavation proceeds with I18 I-beam supports 80 cm spacing), D25 hollow grouting anchors 3.5 m length, 80 × 100 cm spacing), Φ8 mm reinforcing mesh 20 × 20 cm spacing), and shotcrete applied to a thickness of 24 cm to ensure stability and compressive strength.

ii.Construction Scheme for the Intersection of the Enlarged Contact Duct Section and the Underground Wind Turbine Room:

The initial stages align with the equipment transport channel plan, prioritizing the wind turbine room's support. Steel arches are installed, and shotcrete is applied to 13 cm half design thickness). During inverted arch and secondary lining construction, the enlarged contact duct section is reserved, and excavation begins only after the wind turbine room's secondary lining reaches 100% strength.

Excavation follows the contact duct's contour, removing steel arches and shotcrete manually and mechanically. I32 gantries are installed, and pre-support conduits are positioned as shown in Fig. 19. Double rows of advanced grouting conduits 4.0 m length, 40 cm spacing.are used, along with I20a I-beams spaced 50 cm apart. D25 hollow grouting bolts 4.0 m length.are staggered at 50 × 50 cm intervals, reinforced with double layers of Φ8 mm steel mesh 20 × 20 cm spacing). Shotcrete is applied at 26 cm overall thickness, with 13 cm reserved for the intersection area [14].

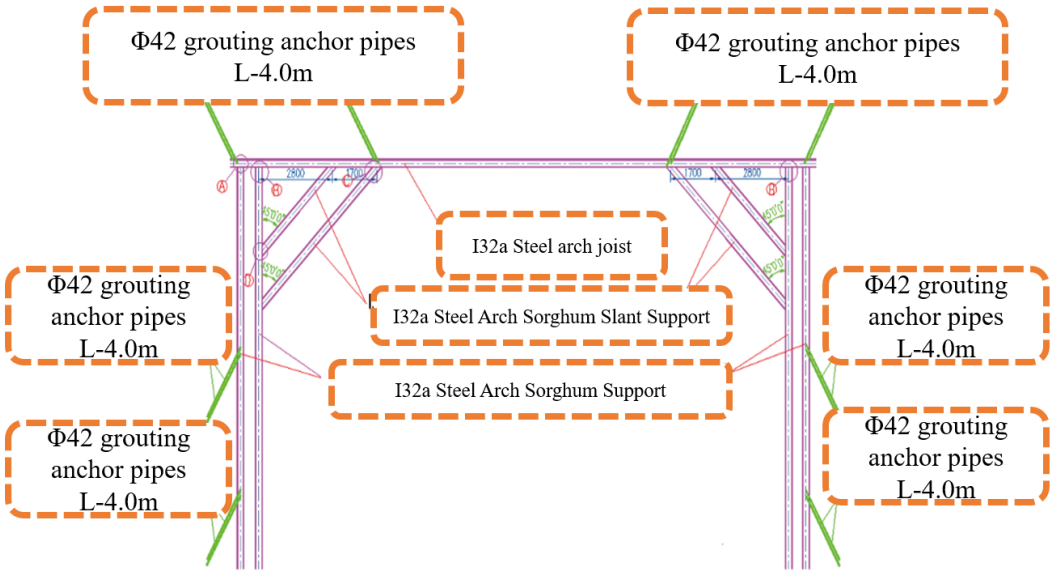


**Figure. 18 Structural diagram of support beams for the expanded section of the underground wind turbine room and the left and right line liaison ducts.**

iii. Construction program for the intersection of the left line contact duct and the left line of the main line:

After completing the initial support for the main-line left line, the intersection with the left-line contact duct is constructed. Initial support includes erecting steel arches and applying shotcrete to half the design thickness 12 cm). Once the main-line left-line initial support extends to MLK3+158, intersection excavation begins.

Before excavation, steel arches and shotcrete within the contour line are removed, followed by installing I32 gantries and overrun conduits. After completing pre-support work, formal excavation begins. The support system uses 42 mm overrun grouting small conduits, 4.0 m in length and spaced 40 cm apart, arranged in the arch's 120° zone. I18 I-beams are spaced 60 cm apart, and D25 hollow grouting anchors 3.5 m length, 60 × 100 cm spacing.are arranged in a plum-blossom pattern. Reinforcement includes Φ6 mm steel mesh with 20 × 20 cm spacing. Shotcrete is applied at 24 cm thickness, with 12 cm in the intersection area.

iv.Construction program for the right line contact duct and main line right line intersection:

Once the main-line right-line initial support is completed, intersection construction begins. Initial support involves steel arch installation and shotcrete application to half the designed thickness 13 cm). Excavation and support proceed to MRK3+160 after the main-line left-line second lining reaches MLK3+150 and the section spanning MLK0+195 to MLK0+205 achieves 100% design strength.

Intersection excavation involves removing steel frames and shotcrete along the contour line, followed by I32 gantry setup and overrun conduit installation. The support system features 50 mm overrun grouting small conduits 4.0 m length, 40 cm spacing.positioned at a 120° arch angle. I20a I-beams are spaced 60 cm apart, and D25 hollow grouting anchors 4.0 m length, 60 × 100 cm staggered spacing.provide additional reinforcement. The system includes Φ8 mm steel mesh 20 × 20 cm spacing), with shotcrete applied at 26 cm thickness, including 13 cm at the intersection.

## V. CONCLUSION

This paper explores the optimization of excavation sequences, support schemes, and lining construction time nodes to ensure the safety and efficiency of complex tunnel projects. By analyzing the construction characteristics of the multiple bifurcation intersections in the underground wind turbine room of the Suzhou International Rapid Logistic Corridor Phase II Project, combined with three-dimensional finite element numerical simulations, the study demonstrates that a well-designed construction sequence and technical approach can effectively reduce surrounding rock deformation, control tunnel settlement, and minimize construction risks.

i.The study shows that the excavation sequence from a large section to a small section large-expansion-small construction method.can significantly reduce the displacement of unexcavated soil, especially in the intersection area, where the deformation of surrounding rock is significantly reduced, and the stability of the support system is enhanced. This optimization method is especially important at intersections with frequent changes in complex sections, where the stress concentration phenomenon of local surrounding rocks can be better controlled by appropriate construction sequences to reduce the range of possible damage.

ii.The effects of different lining sequences on tunnel deformation and settlement were studied and compared. The results show that the lining program immediately after the wind turbine room excavation is completed is better than the lining method after the completion of the pipeline system construction, as it can more effectively control the overall displacement, especially in the wind turbine room where the lower soil settlement control effect is remarkable. Through the reasonable arrangement of lining construction, the secondary deformation of the surrounding rock and the uneven forceon the supporting structure can be reduced, further improving the overall stability of the tunnel structure.

iii.The study shows that the effect of the construction of the up-span right-line ventilation duct on the settlement of the left-line span tunnel is more obvious, especially in the soil and surface area around the left-line tunnel, where the increase in settlement is more significant. Therefore, during the construction of the right-line ventilation duct, it is necessary to strengthen the design and monitoring of the support around the left-line tunnel and take more stringent construction control measures to minimize the impact on existing structures. This finding provides a technical reference for the construction of similar large-span tunnels and multi-lane intersections.

iv.By combining the analysis of actual construction methods, this study proposes optimized construction sequences, support designs, and lining strategies, which provide practical references for the construction of similar complex tunnel structures. This not only helps to reduce the deformation of surrounding rocks and structures during construction but also improves overall construction efficiency and ensures the safety and longevity of the project.

## REFERENCES


[1]. Li T P. Study of highway roadbed, bridge and tunnel interface schemes [J]. Transport Manager World, 2024, 02): 89-91.

[2]. Zhang Z Q, Xu J, Wan X Y. Study on tunnel construction mechanics at intersection of horizontal adit and major tunnel in highway [J]. Rock and Soil Mechanics, 2007, 02): 247-252.

[3]. Li C Y,Stability analysis of the surrounding rocks of underground plant cavern group of BTK hydropower station[D]. Xi'an University of Technology,2022.

[4]. Luo Y B,Chen J X, Wang M S.Study on the Influence of Skew Horizontal Adit Tunnel Construction on Main Tunnel Lining Structure[J]. Journal of Rock Mechanics and Geotechnical Engineering, 2010, 29S2): 3792-3798.

[5]. Yang L D, Deng T,Chen H J.Stability analysis of Longtan Hydropower Station underground plant at the intersection of main branch holes[J]. Chinese Journal of Underground Space and Engineering.2005, 05): 679-684.

[6]. Pan T. Study on peripheral rock stability and support design of underground cavern group of Yellow River Zihaxia Hydropower Station [D]. Xi'an University of Technology, 2016.

[7]. Kan C, Zhang Z H, Guo Y H, et al. Study on Mechanical Characteristics of SFRC Lining at Intersection of Inclined Well and Tunnel [J]. Chinese Journal of Underground Space and Engineering, 2014, 1006): 1387-1393.

[8]. Zhang Z G,Zhang M X. Deformation Prediction of Subway Tunnel Induced by EPB Shield in Soft Clay During Above and Below Overlapping Traversing Process and Its Construction Control[J]. Journal of Rock Mechanics and Geotechnical Engineering, 2013, 32S2): 3428-3439.

[9]. Gao D. Safety Assessment of Ventilation Structures in Chikangam Tunnel, 2014, 5901): 236-240.

[10]. Zhou Y P. Analysis of ground stress characteristics and stability of surrounding rocks in deeply buried hydraulic tunnels [D]. ShiHeZi University, 2022.

[11]. Ping X Z , Hui S T , Sheng Q L, et al.Key technology for the construction and inspection of long-distance underwater tunnel for 1000 kV gas-insulated transmission line[J]. Bulletin of Engineering Geology and the Environment, 2022, 821).

[12]. Rauch F , Oreste P , Fischer O . Internal forces measured in segmental tunnel linings compared with numerical predictions obtained from state-of-the-art calculation methods used in engineering practice[J]. Tunnelling and Underground Space Technology incorporating Trenchless Technology Research, 2024, 154106084-106084.

[13]. Chai S , Yan Y , Hu B , et al.The Optimization of Secondary Lining Construction Time for Shield Tunnels Based on Longitudinal Mechanical Properties[J]. Applied Sciences, 2023, 1319):

[14]. Wang Q , Wei H ,Jiang B , et al.High pre-tension reinforcing technology and design for ultra-shallow buried large-span urban tunnels[J]. International Journal of Rock Mechanics and Mining Sciences, 2024, 182105891-105891.

[15]. Wen X G , ShuaiQing L , Yang B J , et al.Intelligent crack damage detection system in shield tunnel using combination of retinanet and optimal adaptive selection[J]. Journal of Intelligent & Fuzzy Systems, 2021, 403): 4453-4469.